



III Всероссийская научная конференция
«ВОЛНЫ ЦУНАМИ: МОДЕЛИРОВАНИЕ, МОНИТОРИНГ, ПРОГНОЗ»
Москва, 16-17 ноября 2021 г.

Применение метода R-решения при проектировании размещения
системы наблюдения за цунами

Воронина Т. А

Институт вычислительной математики и математической геофизики СО РАН,
Новосибирск, vta@omzg.sccc.ru



The forward problem (FP)

$$\eta_{tt} = \nabla^T (gh(x, y) \nabla \eta) \quad (1)$$

The initial conditions:

$$\eta|_{t=0} = \varphi(x, y); \quad \eta_t|_{t=0} = 0 \quad (2)$$

The boundary conditions:

$$\frac{\partial \eta}{\partial \vec{n}} = 0$$

on the solid boundary

on the open boundary

$$-\mathbf{c}\vec{V} \cdot \vec{n} - \eta_{tt} + \frac{c^2 \partial^2 \eta}{2\partial \vec{r}^2}|_{\Gamma} = 0$$

$$\eta(x, y, t)|_M = \eta_0(x_i, y_i, t), \quad M = \{(x_i, y_i), i=1, \dots, P\} \quad (4)$$

$\eta(x, y, t)$ the water elevation above the mean level

$\varphi(x, y) \in \Omega$ the initial sea surface displacement

$c(x, y) = \sqrt{gh(x, y)}$ the wave phase velocity

g the gravity acceleration

$h(x, y)$ the depth of the ocean

$\Omega = \{(x, y) \in [(0, l_1) \times (0, l_2)]\}$ the tsunami source area
 $\Omega \subset \Phi$

$\eta_0(x_i, y_i, t)$ the observed tsunami waveform

The inverse problem is to recover the function $\varphi(x, y)$ from the equation:

$$A\varphi = \eta_0(t)$$

The inverse problem (IP)

The IP is to recover the function $\varphi(x, y)$ from the equation:

$$A\varphi = \eta_0(t)$$

The operator A maps the initial water elevation onto the data $\eta_0(t)$.

Inverse problem data in application

$$\eta_0(t) = (\eta(x_1, y_1, t_1), \eta(x_2, y_2, t_2), \dots, \eta(x_p, y_p, t_p)), M_i = (x_i, y_i), i=1,2,\dots,P$$

singular system of compact operator A :

$(\bar{v}_i, \bar{u}_i, s_i)$ \bar{v}_i, \bar{u}_i are the left and the right singular vectors,

$\{s_i\}$ are its singular values, $i \rightarrow \infty, s_i \rightarrow 0$

$$A\bar{v}_i = s_i \bar{u}_i; \quad \text{i.e. } A = U\Sigma V^T; \quad \Sigma = \begin{pmatrix} s_1 & & \cdots & \\ \vdots & & s_2 & \\ & \cdots & & \ddots \end{pmatrix}$$

$$\varphi(x, y) = \sum_{i=1}^{\infty} \frac{(\bar{\eta}_0 + \bar{\epsilon}, \bar{u}_i)}{s_i} \bar{v}_i, \quad s_i / (\bar{\epsilon}, \bar{u}_i) \rightarrow 0, i \rightarrow \infty, \bar{\epsilon} - \text{data error}$$

r-solution $\varphi^{[r]}(x, y) = \sum_{i=1}^{i=r} \frac{(\bar{\eta}_0 + \bar{\epsilon}, \bar{u}_i)}{s_i} \bar{v}_i$

Regularization: by means of truncated SVD

V.A. Cheverda and V.I. Kostin. "R-pseudo-inverse of a compact operator in the Hilbert spaces //Siberian Electronic Mathematical Reports, vol. 7, pp. 258–282, 2010.

Воронина Т.А. , Определение пространственного распределения источников колебаний по дистанционным измерениям в конечном числе точек, СибЖВМ, 2004, 7, № 3, стр. 203–211.

The algorithm/Discrete inverse problem

$$\varphi(x, y) = \sum_{m=1}^M \sum_{n=1}^N c_{mn} \sin \frac{\pi m}{l_1} x \cdot \sin \frac{\pi n}{l_2} y = \sum_{m=1}^M \sum_{n=1}^N c_{mn} \varphi_{mn}(x, y)$$

$$\Omega = [0, l_1] \times [0, l_2] \quad \bar{c} = \{c_{mn}\}_{m=1, n=1}^{m=M, n=N} ; \quad \bar{\eta}_0 = \{\eta_0(x_p, y_p, t_j)\}, \quad p=1, \dots, P; j=1, \dots, N_t$$

$$A\bar{c} = \bar{\eta}_0$$

The matrix A : $(P \times N_t) \times (M \times N)$; $\eta|_{t=0} = \varphi_{mn}$;

$$A = U\Sigma V^T$$

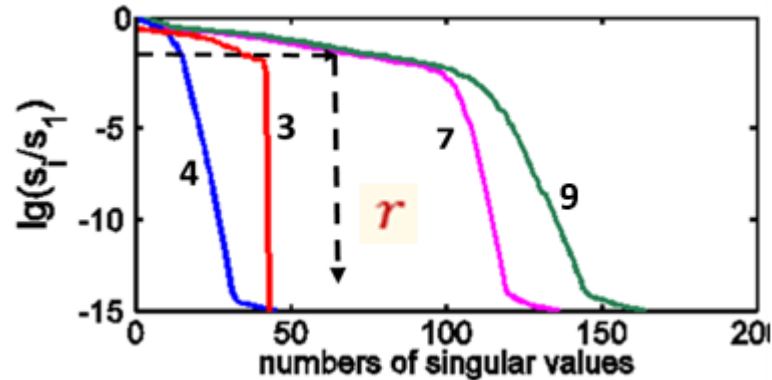
r - solution $\bar{c}^{[r]} = \sum_{j=1}^r \frac{(\bar{\eta}_0 + \bar{\varepsilon}) \cdot \bar{u}_j}{s_j} \bar{v}_j, \quad r = \max \left\{ k : \frac{s_k}{s_1} \geq \textcolor{red}{d} \right\}$

$$\varphi^{[r]}(x, y) = \sum_{j=1}^{j=r} \alpha_i \Phi_i(x, y) = \sum_{j=1}^{j=r} \alpha_i \sum_{m=1}^M \sum_{n=1}^N \beta_{mn}^j \varphi_{mn}(x, y),$$

$$\alpha_i = \frac{(\eta_0 \circ u_i)}{s_i}; \quad \Phi_i(x, y) = \sum_{m=1}^M \sum_{n=1}^N \beta_{mn}^i \varphi_{mn}(x, y); \quad v_i = (\beta_{11}^i, \beta_{12}^i, \dots, \beta_{MN}^i)$$

The inverse problem (IP)

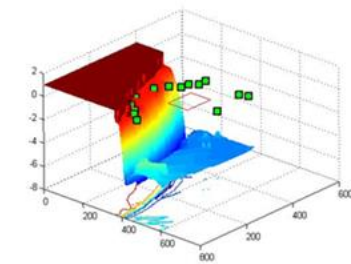
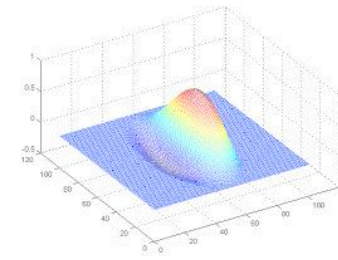
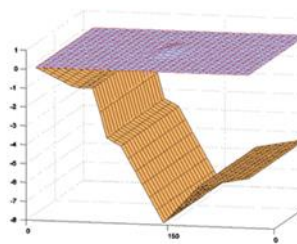
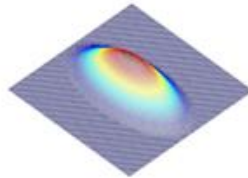
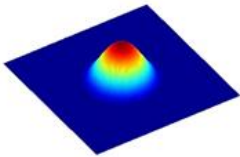
r - solution $\bar{c}[r] = \sum_{j=1}^r \frac{(\bar{\eta}_0 + \bar{\varepsilon}) \cdot \bar{u}_j}{s_j} \bar{v}_j, \quad r = \max \left\{ k : \frac{s_k}{s_1} \geq d \right\}$



Voronina, T. A., Voronin, V. V., and Cheverda, V. A. The 2015 Illapel Tsunami Source Recovery by Inversion of DART Tsunami Waveforms Using the R-Solution Method // Pure and Applied Geophysics. 2019. V.176, №7, C.2985-2993.

Voronina T.A. and Voronin V.V., A Study of Implementation Features of the r-Solution Method for Tsunami Source Recovery in the Case of the Illapel Tsunami 2015 // Pure and Applied Geophysics, 2021, <https://doi.org/10.1007/s00024-021-02843-7>

The model cases



I. $h(x, y) = \text{const}$
background noise 0%
semi-sphere
semi-ellipsoid

- aperture length, its geometry
- frequency band
- receivers-to-source distance
- number of receivers
- aperture angle

II. $h(x, y) = h(x)$
background noise 0%- 5%
sea floor deformation of typical
tsunamigenic earthquakes

- disposition
- number of receivers
- aperture width vs. size of source
- background noise

III. $h(x, y)$ real bathymetry
background noise 0%- 3%
sea floor deformation of typical
tsunamigenic earthquakes

- disposition
- number of receivers
- aperture width vs. size of source
- background noise
- the “most informative” direction

Voronina,T.A., Tcheverda,V.A. 1998, Reconstruction of tsunami initial form via level oscillation, Bull.Nov.Comp.Center, Math.Model.in Geoph., 4, 127-136,

T. A. Voronina, 2002 “Reconstruction of initial tsunami waveform by the coastal observations inversion,” Bull.NCC, Math.Model.in Geoph., vol. 7, pp. 89–100

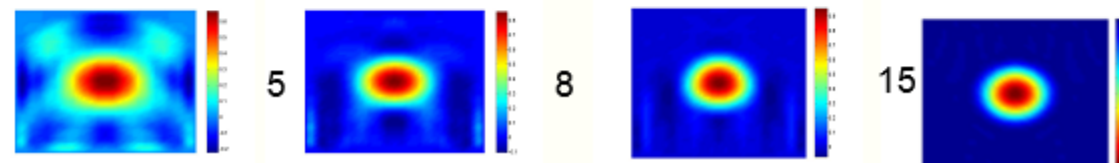
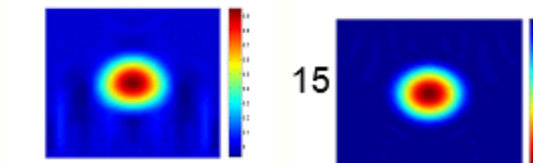
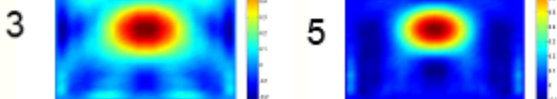
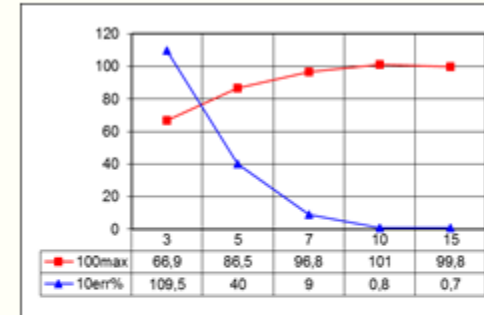
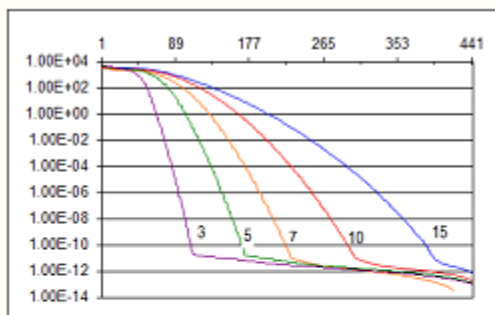
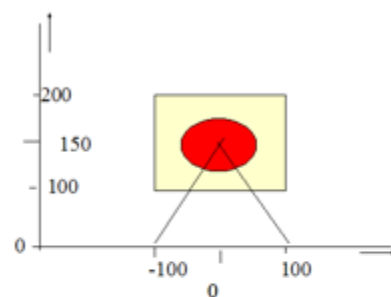
Voronina T.A., Tcheverda V.A., and Voronin V.V. 2014, Some properties of the inverse operator for a tsunami source recovery // Siberian Electronic Mathematical Report, Vol. 11, P. 532–547.

Voronin,V.V., Voronina,T.A., and Tcheverda,V.A.,(2015), Inversion method for initial tsunami waveform reconstruction, Nat. Hazards Earth Syst. Sci., vol. 15, pp. 1251-1263.

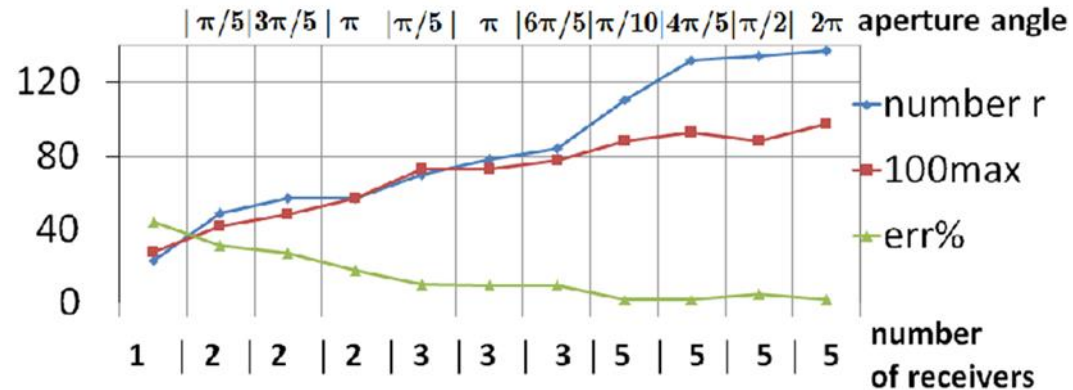
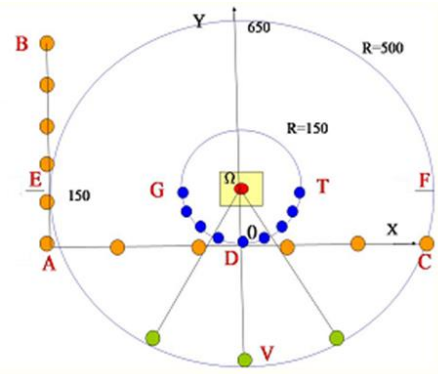
$h(x,y)=const$

- receivers-to-source distance
- aperture angle
- number of receivers

Semi-ellipsoid $R_x = 25$; $R_y = 50$; $L = 200$

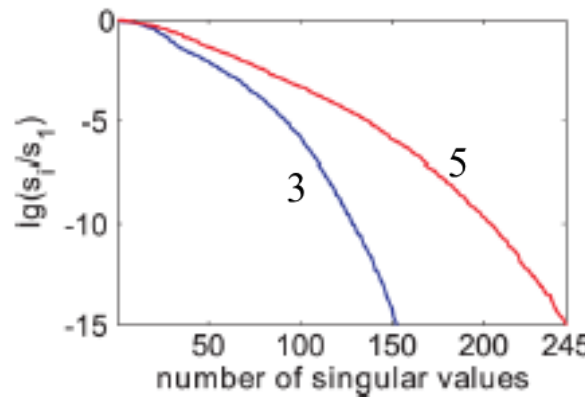
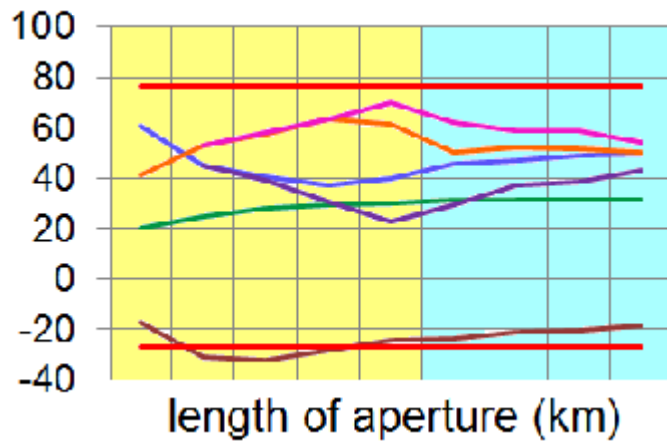
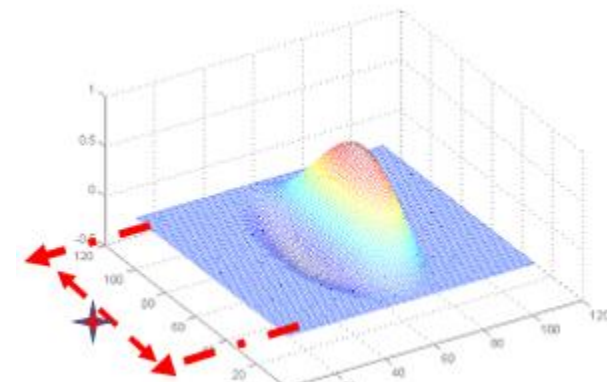
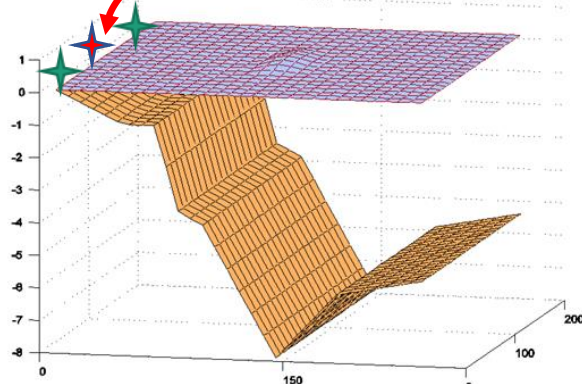


The quality of solution is improving when number of stations increases up to 10-15. The further increase is useless.



I. $h(x,y)=h(x)$

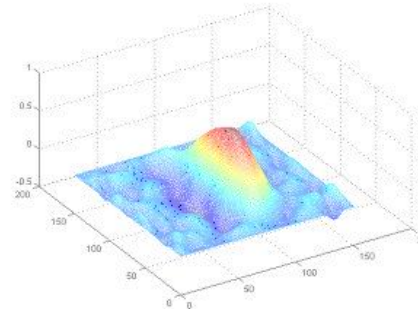
receivers midpoint



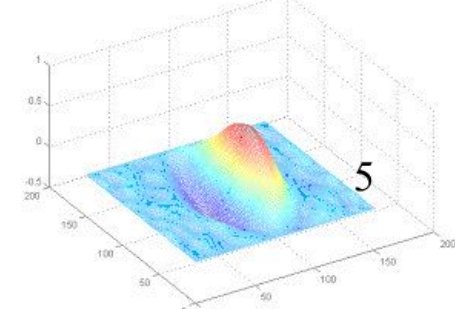
max = 0.73m;
min = 0.34m

max = 0.63m
min = 0.28m

max = 0.71m
min = 0.29m

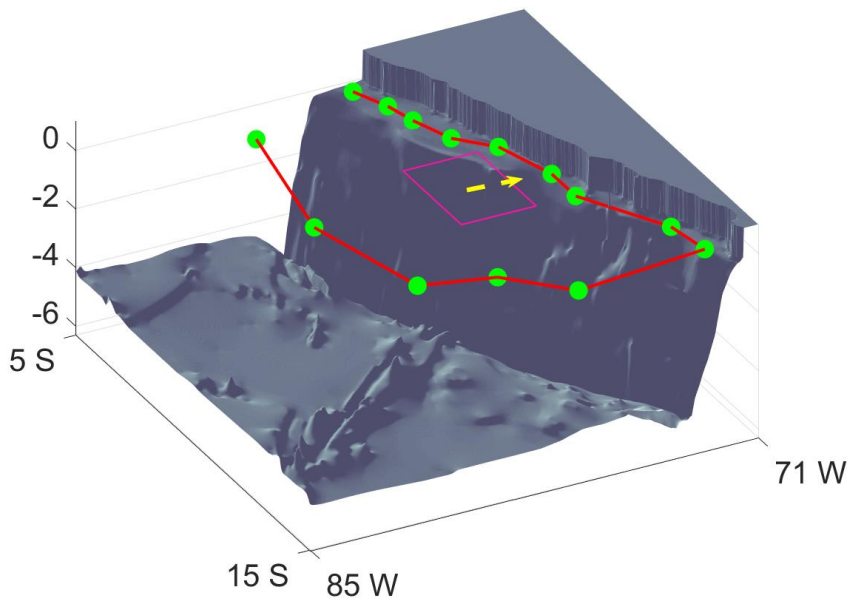


3

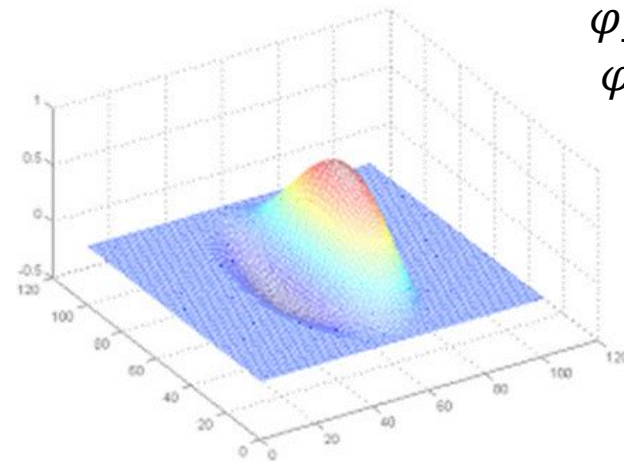


5

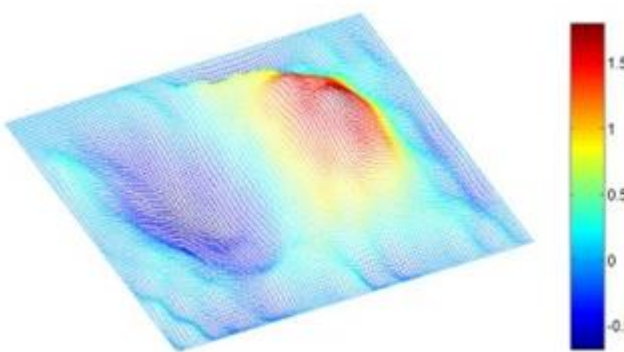
Theoretical –red; Inversion with 3 marigrames: max{ $\varphi(x; y)$ } – orange; err% - blue. Number r- green;
Inversion with 5 marigrames: max{ $\varphi(x; y)$ } –pink;
min{ $\varphi(x; y)$ } –brown; err% - violet.



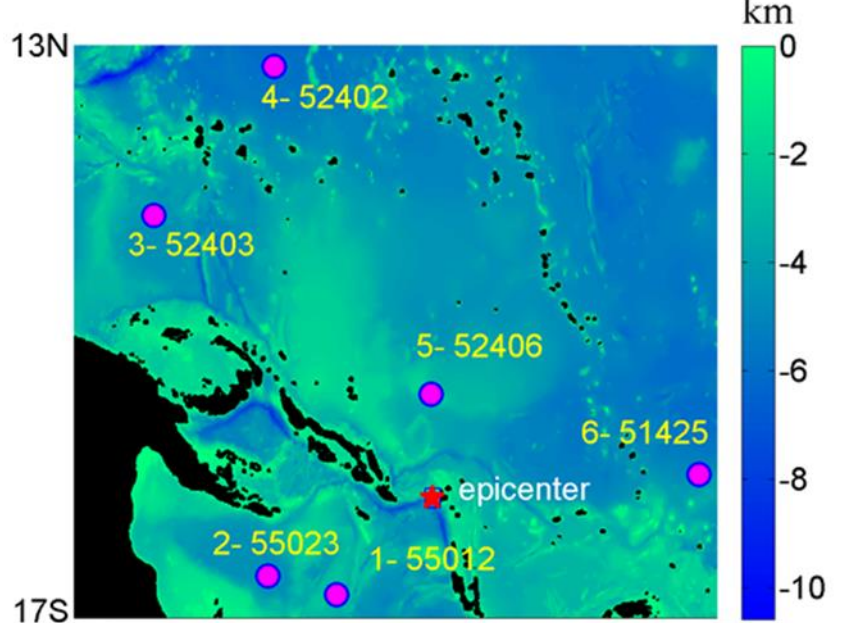
$\varphi_{max}=1.959;$
 $\varphi_{min}=-0.67$



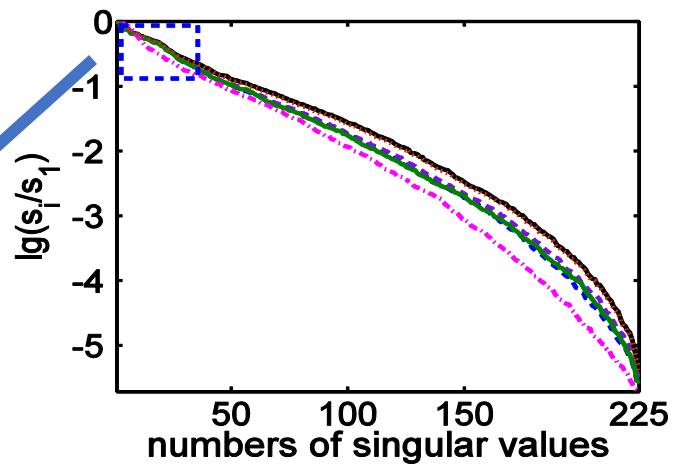
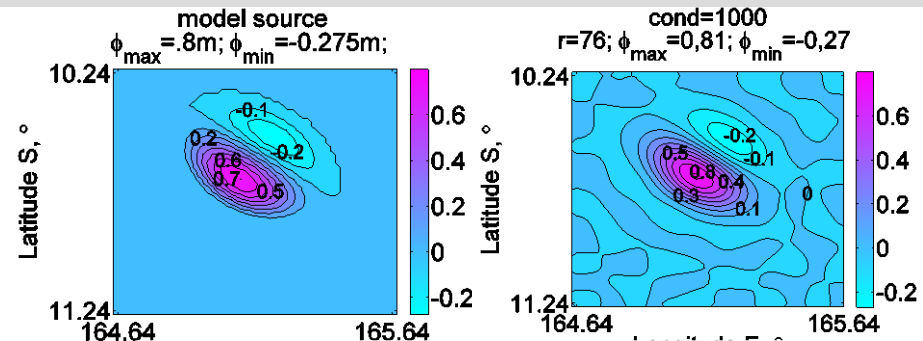
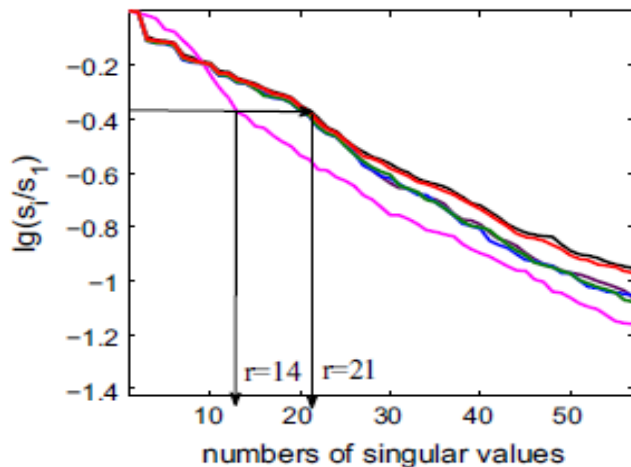
$\varphi_{max} = 1.835m;$
 $\varphi_{min}=-0.702m;$
 $r = 103;$



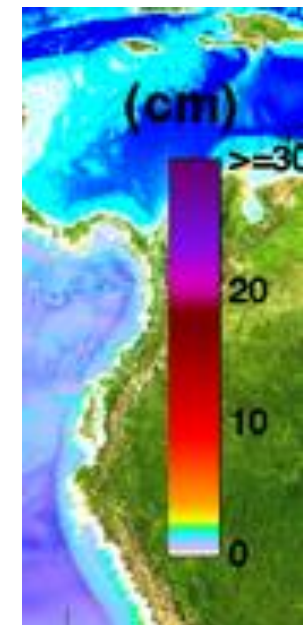
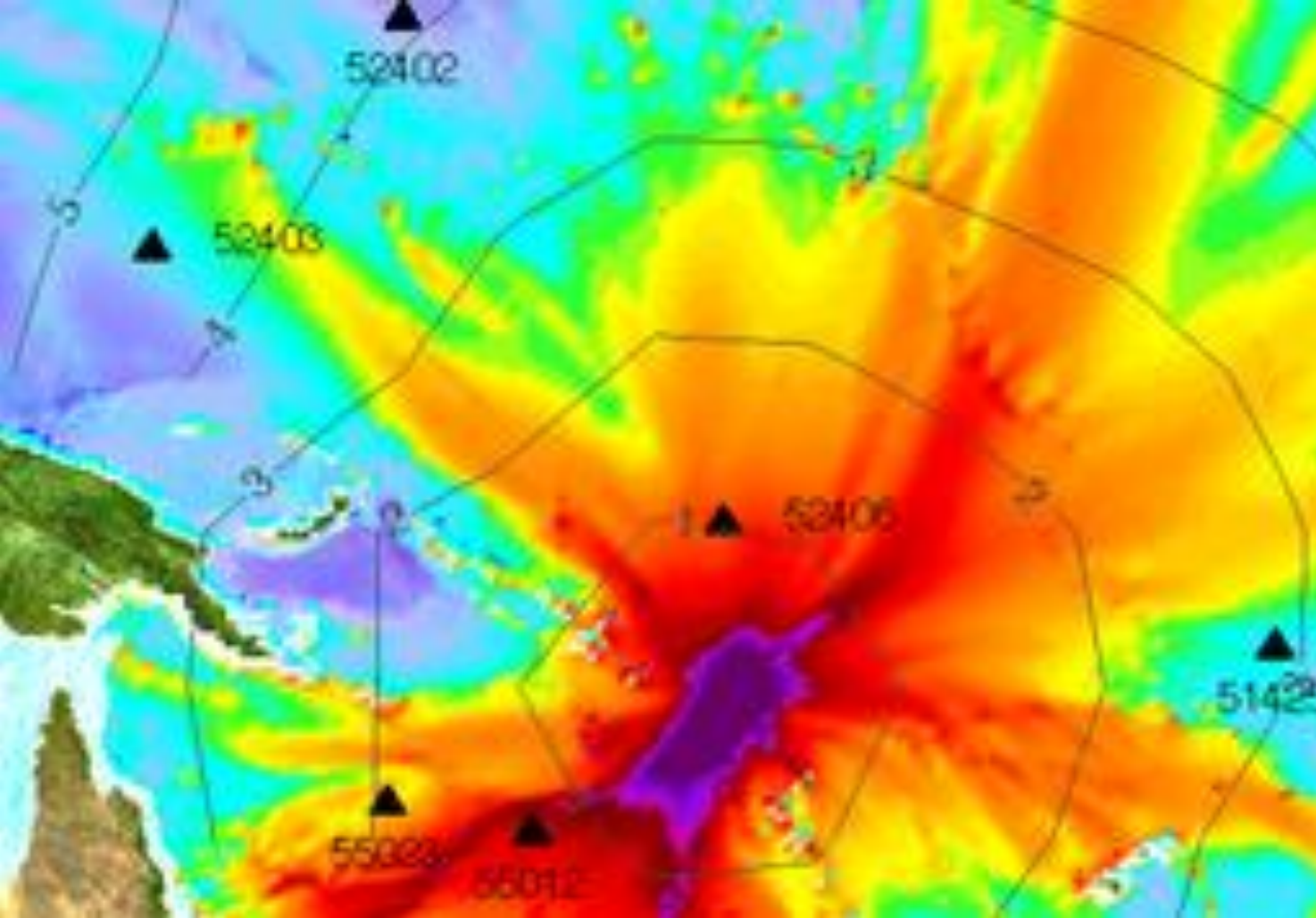
Case study: 2013 Solomon Islands Tsunami



Singular spectra of matrix A (enlarged image)



Graphs of singular values in the common logarithm scale of the matrix A obtained in the inversion with the different sets of the receivers :
 $\{4, 5, 6\}$ (magenta), $\{1, 2, 5\}$ (dark magenta), $\{1, 3, 5\}$ (blue),
 $\{1, 5, 6\}$ (green), $\{1, 2, 3, 5, 6\}$ (red) and
 $\{1, 2, 3, 4, 5, 6\}$ (dark blue).

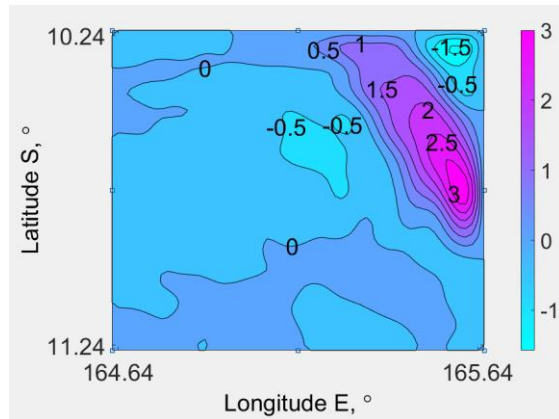
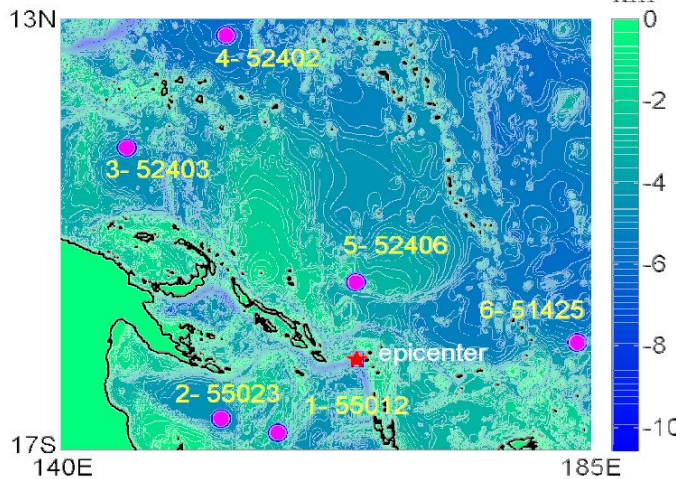


• Model amplitudes calculated with the MOST forecast model. Filled colors show maximum computed tsunami amplitude in cm during 24 hours of wave propagation. Black contours show computed tsunami arrival time.

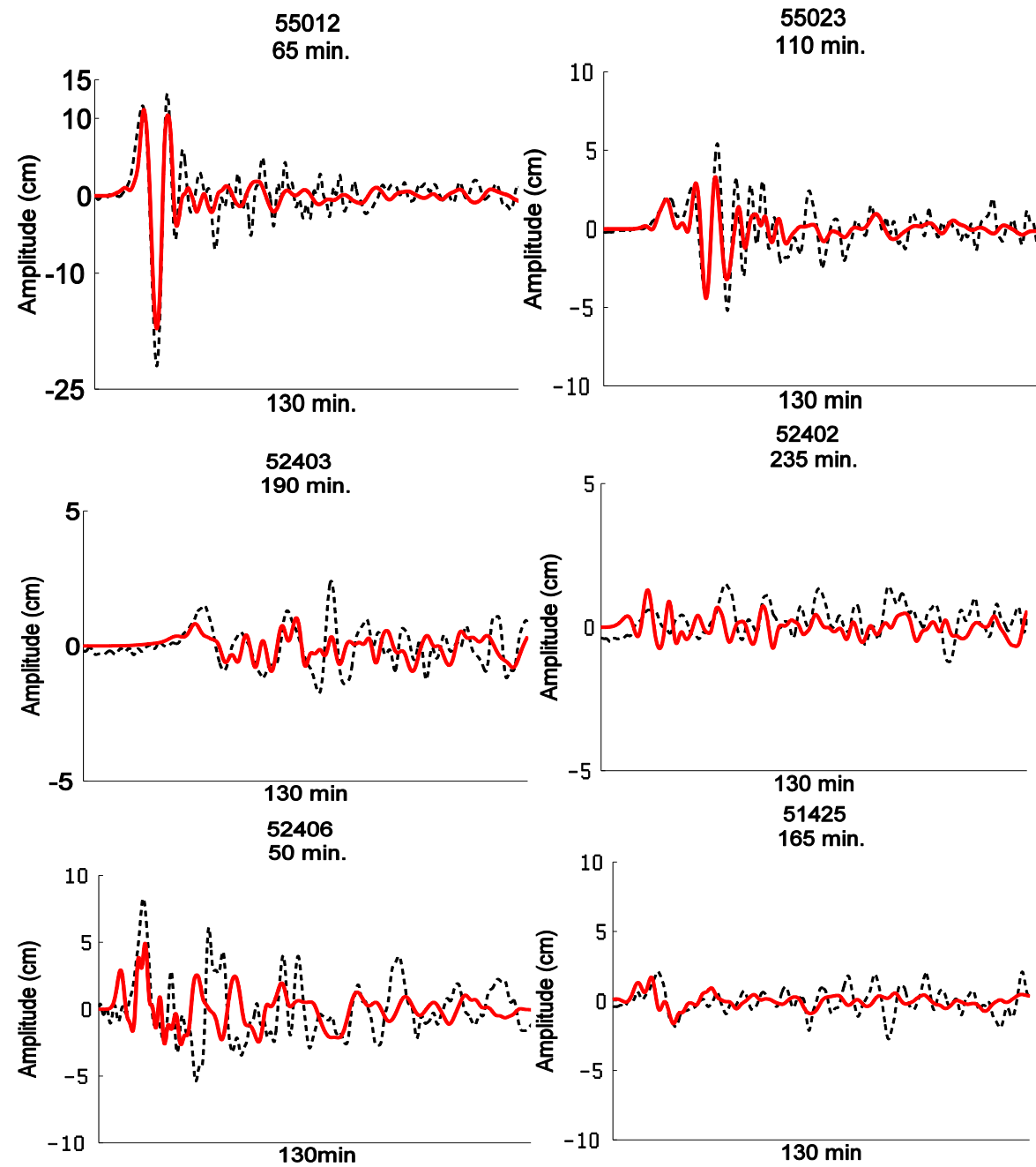
[Titov, V.V., F.I. González, E.N. Bernard, M.C. Eble, H.O. Mofjeld, J.C. Newman, and A.J. Venturato](#) **Real-time tsunami forecasting: Challenges and solutions** *Nat. Hazards*, 35(1), Special Issue, U.S. National Tsunami Hazard Mitigation Program, 41–58 (2005)

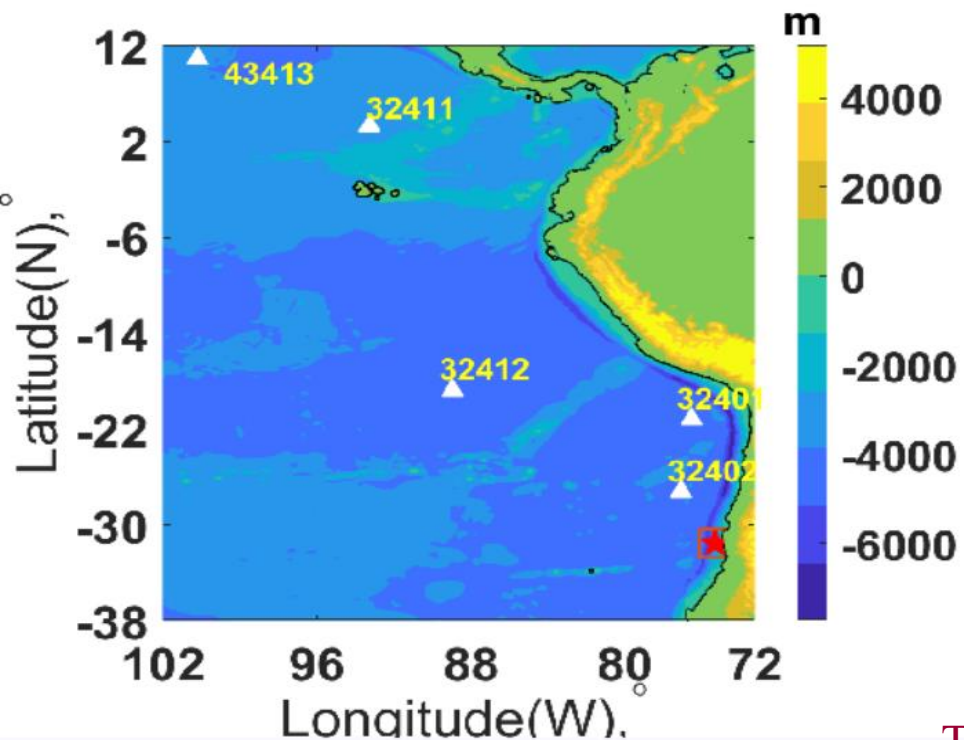
4. Application to Solomon Islands

Tsunami 6 February, 2013

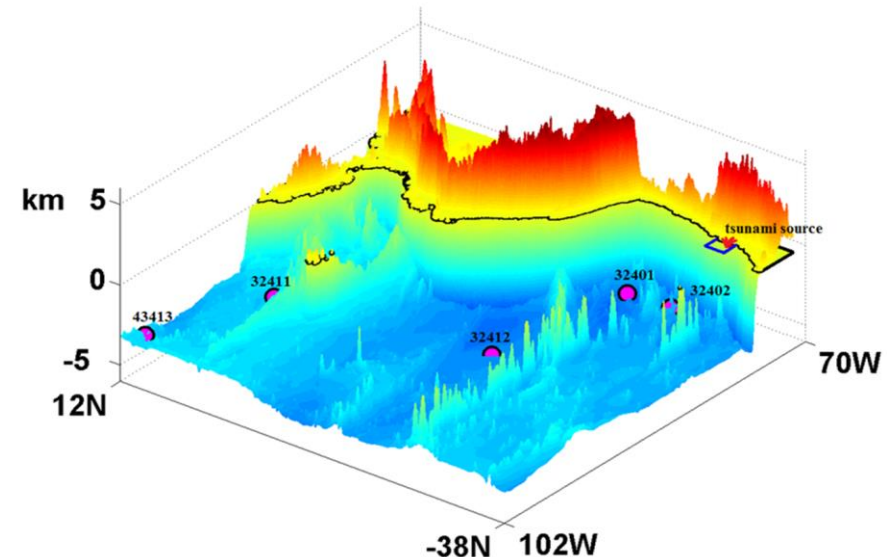
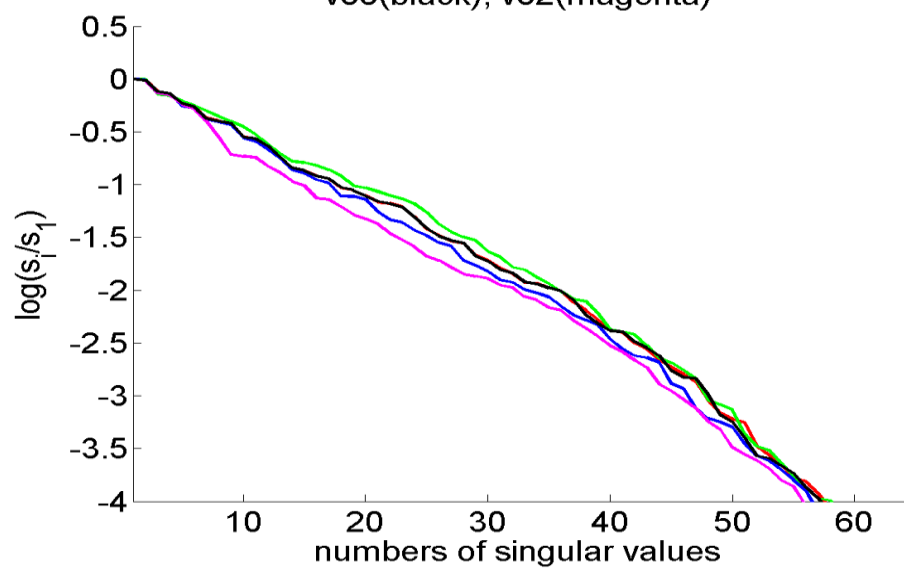


Comparison of observed marigrams (the black line) and calculated ones with five receivers numbered {1, 2, 3, 5, 6} (the red line) of the 2013 Solomon Islands tsunami.



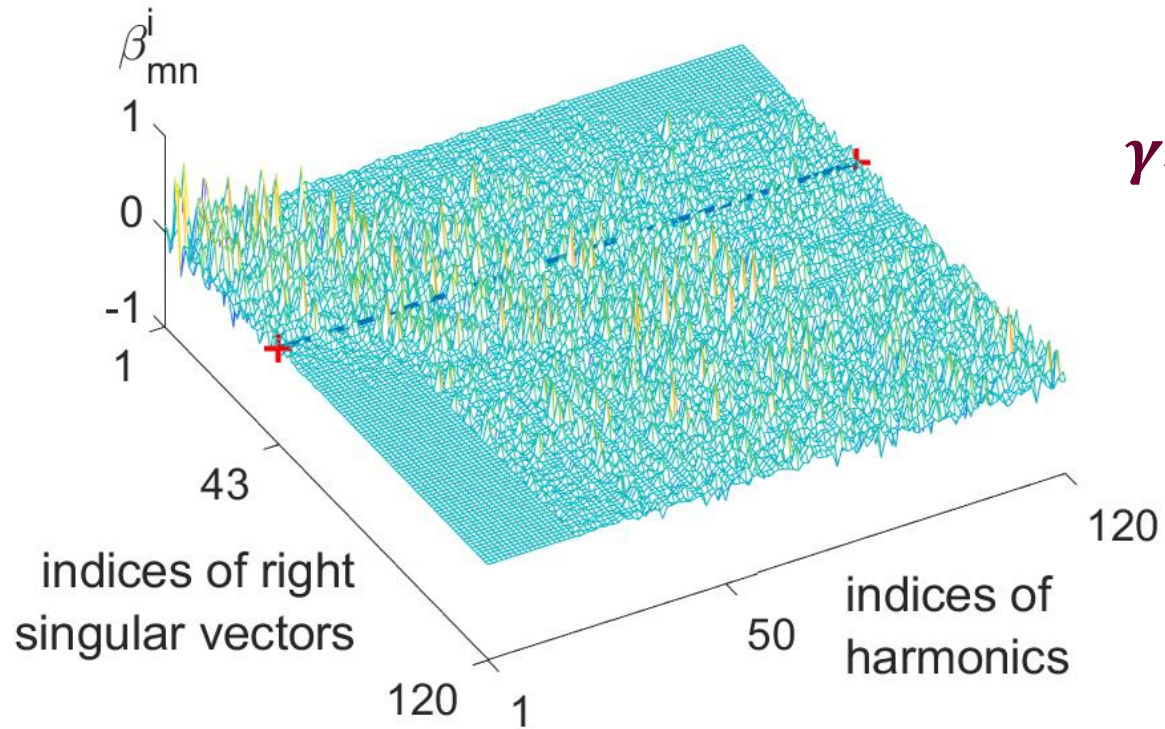


v80(green); v79(red); v81(blue);
v83(black); v82(magenta)

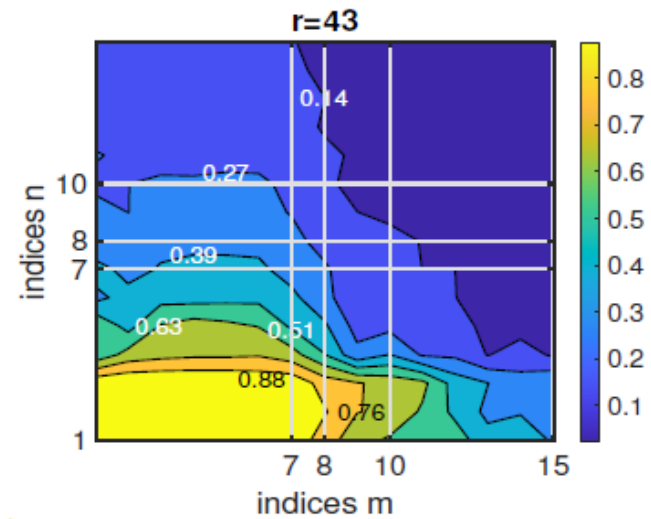


There are the numbers of DART buoys:
1-32402; 2-32401; 3-32412; 4-32411;
5- 43413.

$d=0.02$; $k=88$;
V80(green) C2345; $r=31$;
V79 (red) C1234; $r=29$;
V81(blue) - C1345; $r=25$;
V83 (black) C1235; $r=27$;
V82(magenta) - C1245; $r=25$;

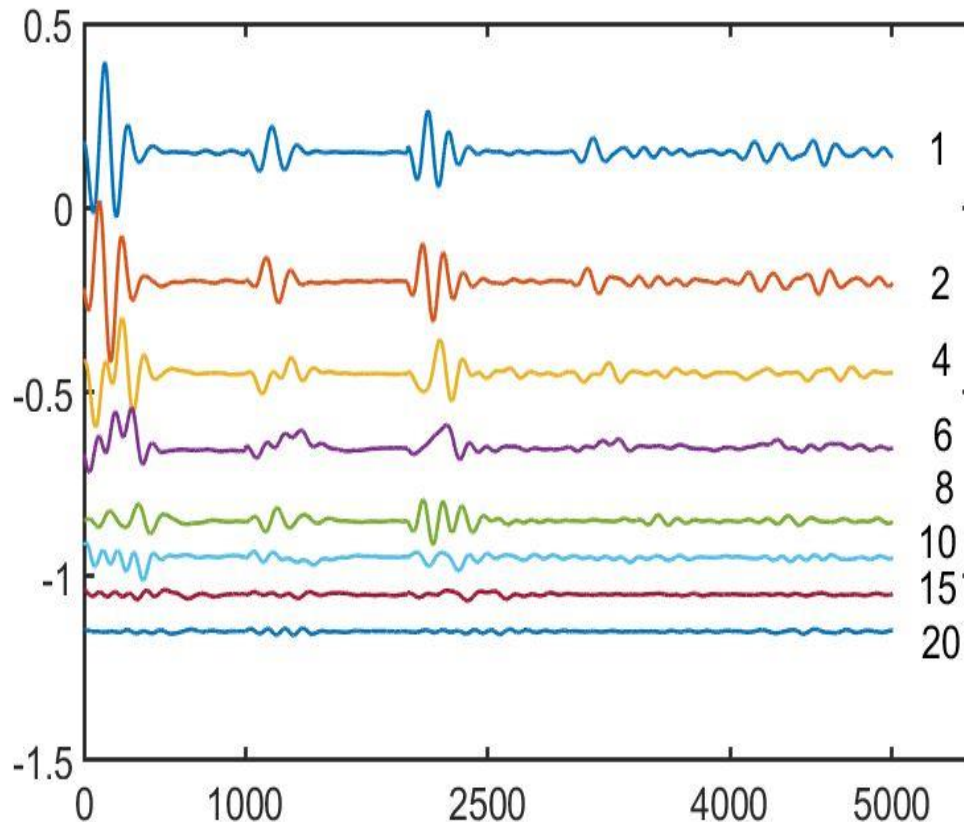


$$\gamma_{mn} = (m/l_1)^2 + (n/l_2)^2$$



The cosine of the angle between each harmonic and a subspace of r -solutions, $r=43$

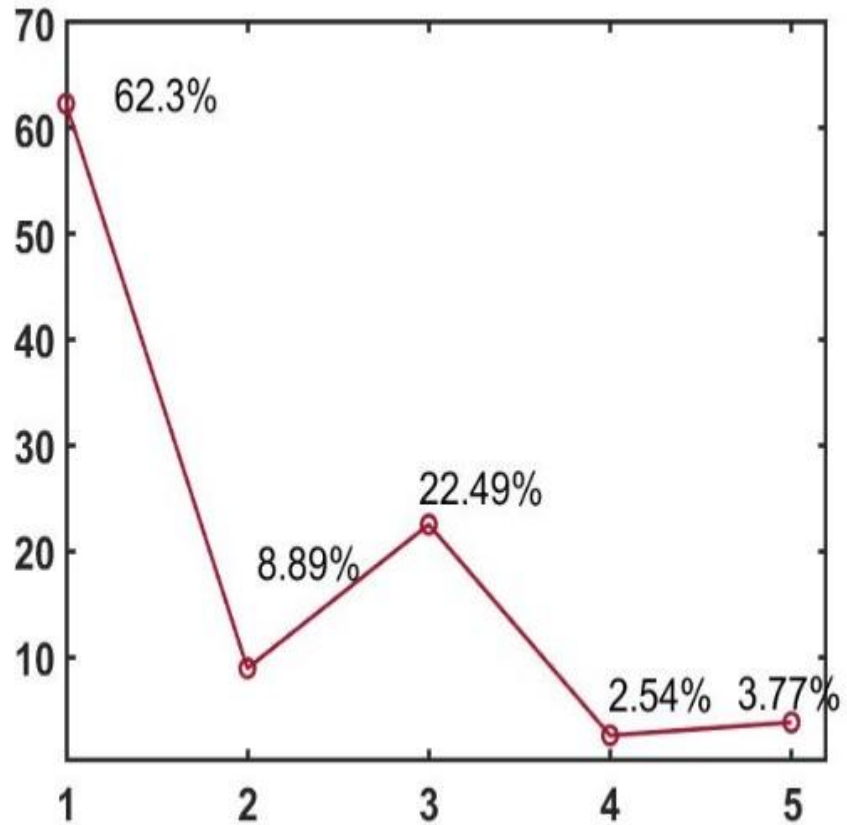
Voronina T.A. and Voronin V.V., 2021 A Study of Implementation Features of the r -Solution Method for Tsunami Source Recovery in the Case of the Illapel Tsunami 2015, *Pure and Applied Geophysics* <https://doi.org/10.1007/s00024-021-02843-7>



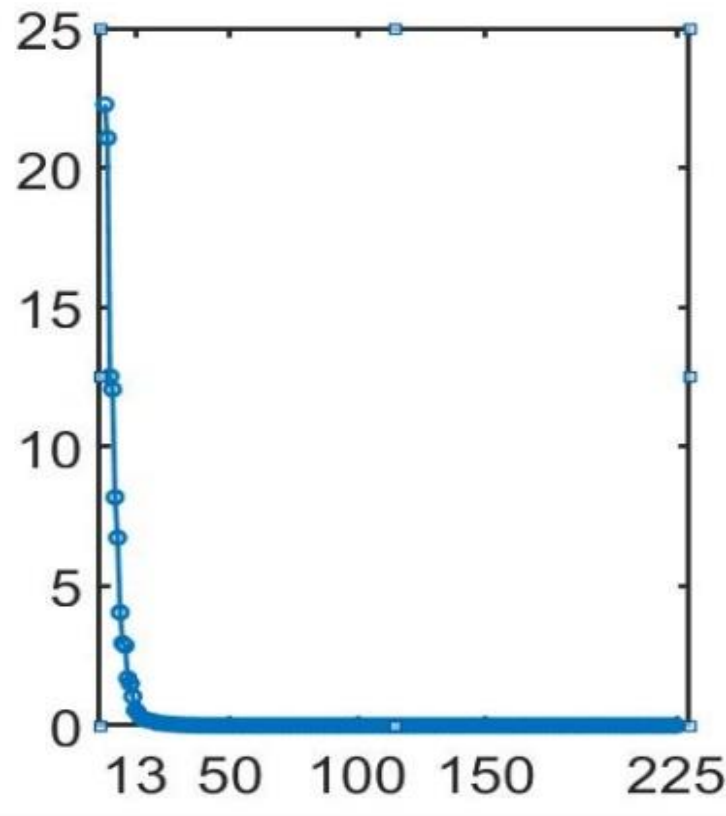
$$\mathbf{A}\bar{\mathbf{v}}_i = \mathbf{s}_i\bar{\mathbf{u}}_i;$$

$\bar{\mathbf{v}}_i, \bar{\mathbf{u}}_i$ are the left and the right singular vectors,
 $\{\mathbf{s}_i\}$ are singular values
 $i \rightarrow \infty, s_i \rightarrow 0$

In this example: the number of the tsunami sensors $P = 5$; 1-minute rectangular grid 1921×3001 in the entire simulation area, the bathymetry is according to GEBCO <http://www.gebco.net/> counts in time $N_t = 1005$ with an interval of 4 seconds; the matrix \mathbf{A} has 225×5005 dimensions, where $M = 15; N = 15; M \times N = 225; P \times N_t = 5005$.

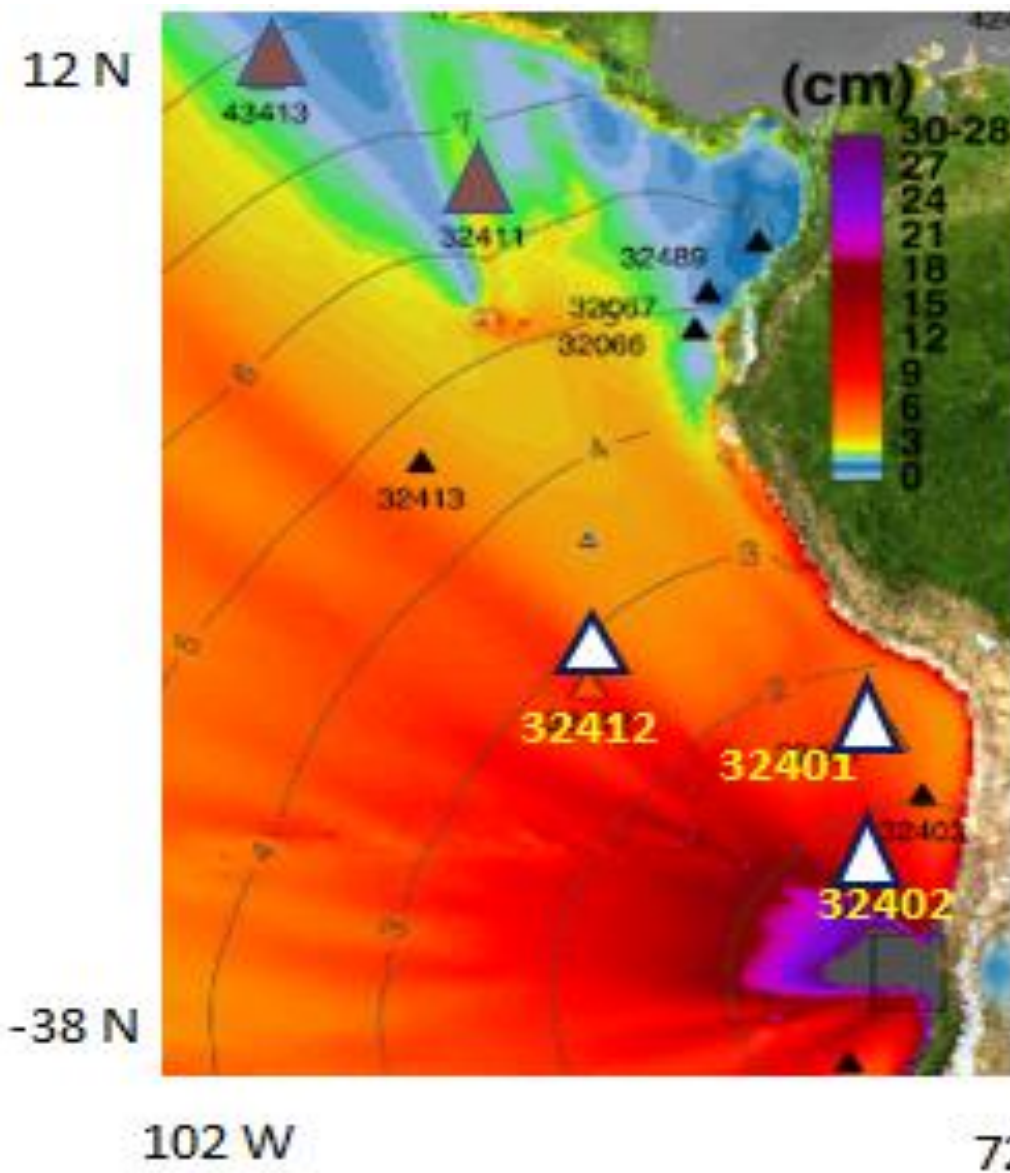


Tsunami wave energy distribution in percentage between the DART buoys used in the inversion. There are the numbers of DART buoys on the horizontal axis: 1-32402; 2-32401; 3-32412; 4-32411; 5-43413.

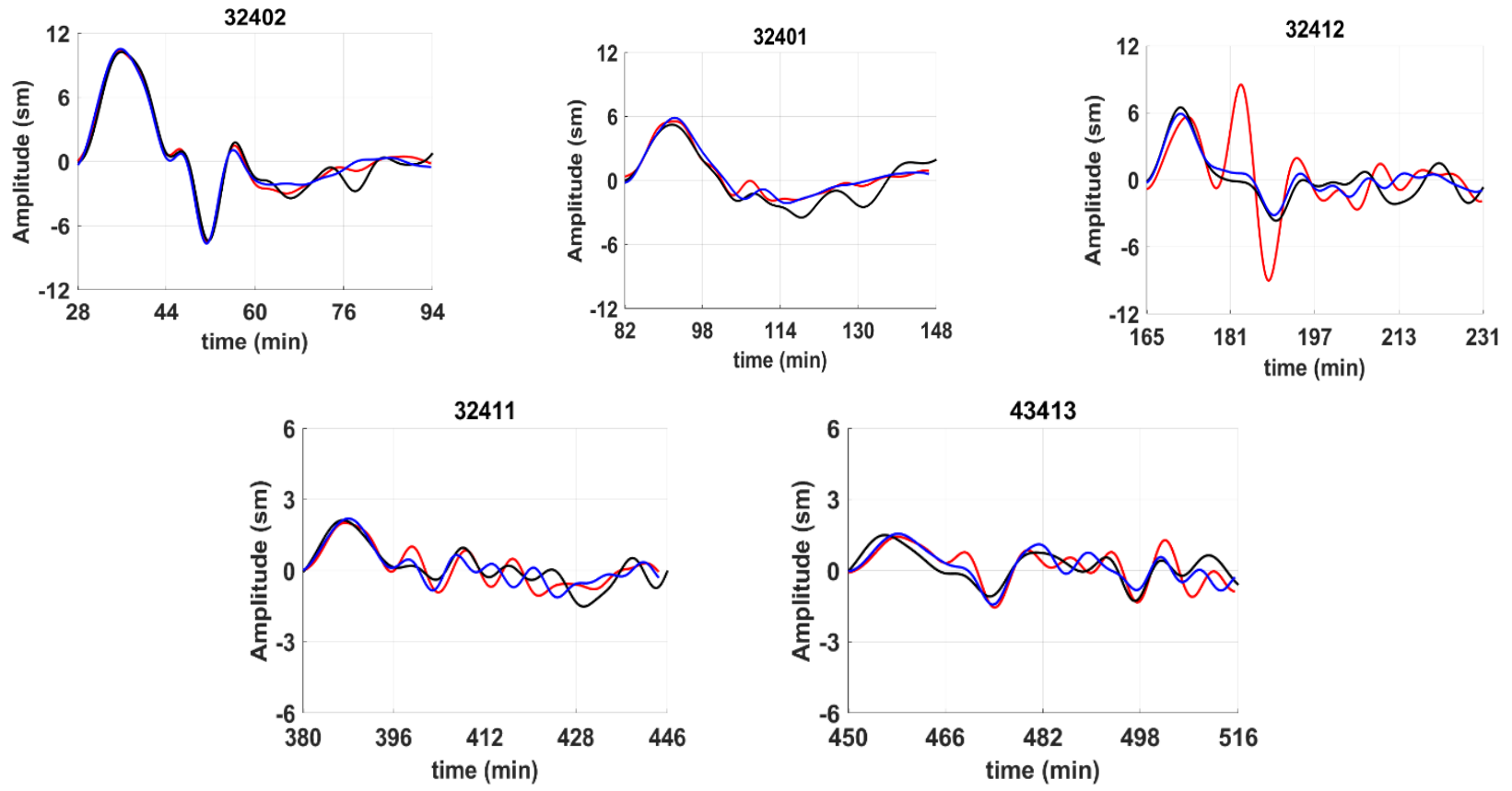


Distribution in the percentage of the energy carried by each mode; the horizontal axis represents the indices of modes.

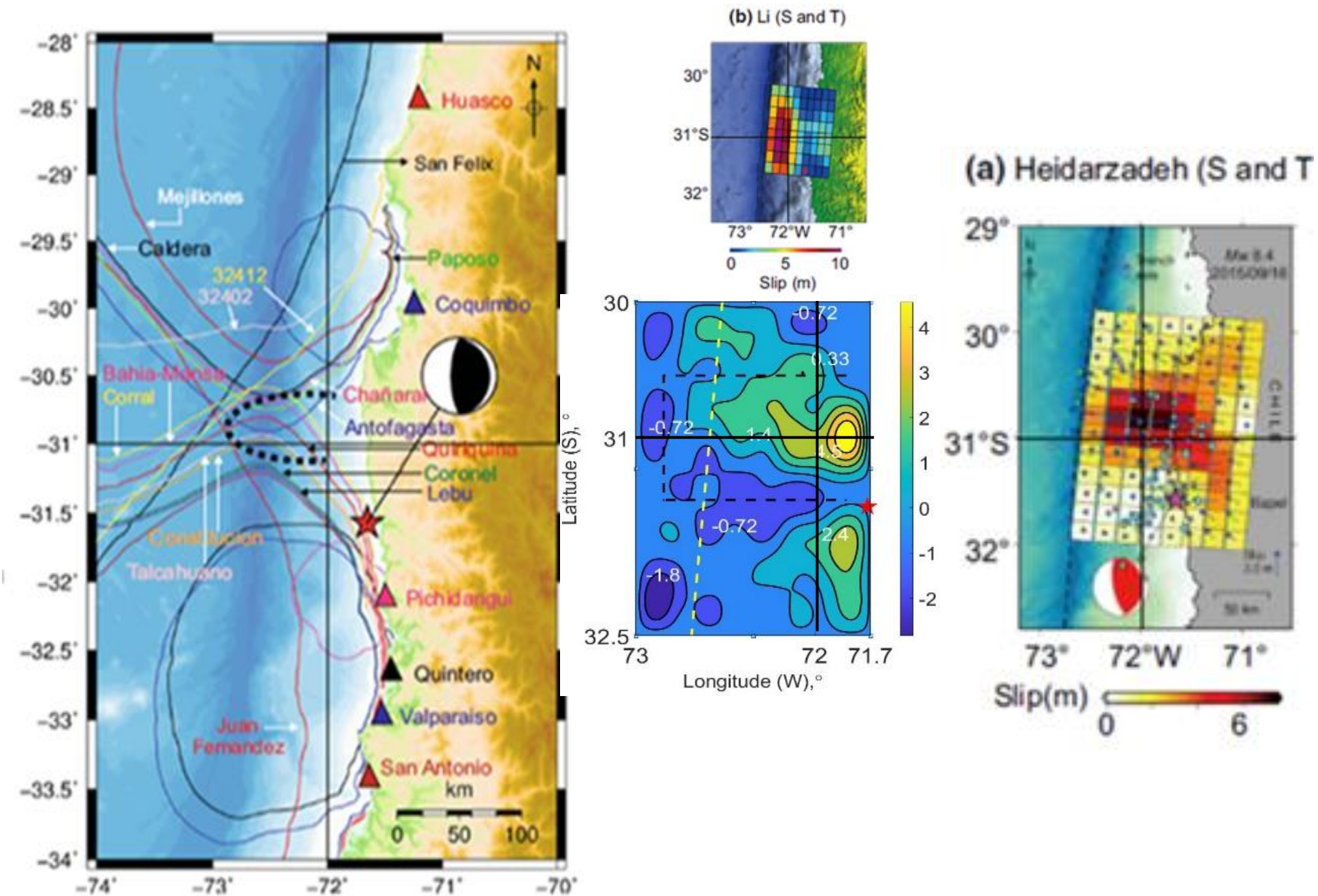
$$\frac{s_i^2}{\sum_i s_i^2}, i = 1, \dots, 225$$



A distribution of the energy of the Illapel tsunami wave of September 16, 2015, according to Tang L, Titov VV, Moore C and Wei Y 2016 Real-Time Assessment of the 16 September 2015 Chile Tsunami and Implications for Near-Field Forecast *Pure and Applied Geophysics* **17** pp 369 – 367; the triangles denote DART buoys.



A comparison of the observed tsunami waveforms (the black lines) and those reconstructed ones with participation of the data of DART buoys 32401 and 32402 (the red lines) and the tsunami waveforms reconstructed when the data of DART buoy 32412 (the blue lines) are added to the inversion with the above ones. On the axis Ox - the time from the beginning of the event.



Satake, K. and Heidarzadeh, M. A. (2017). Review of Source Models of the 2015 Illapel, Chile Earthquake and Insights from Tsunami Data. *Pure Applied Geophysics*, 174, 1-9.

Заключение

Для достоверного восстановления источника цунами и метеограмм в рамках предложенного подхода надо использовать данные глубоководных датчиков уровня поверхности океана от наиболее информативной части системы наблюдения.

В настоящей работе предложена методика поиска наиболее информативной части системы наблюдения, использование которой не только повышает точность восстановления, но и обеспечивает без дополнительных расчетов, вычисление высот волн в любых, заранее фиксированных точках акватории.

Численные эксперименты с модельными системами наблюдения на этапе предварительных расчетов для зон прогнозируемой цунами опасности могут быть обоснованием для планирования размещения глубоководных датчиков.

Такие датчики располагаются на направлениях наиболее интенсивного распространения энергии цунами.

Voronina T.A. ,(2004), Determination of the spatial distribution of the oscillation sources by the remote measurements on a finite set of points, Sib. J. Calc. Math.,7(3),pp. 203-211 (rus). Cheverda V.A. and Kostin V.I., (2010), r-pseudoinverse for compact operator, SEMR,v.7, p258=282.

Voronina, T. A., Tcheverda, V.A., and Voronin, V. V. ,(2014), Some properties of the inverse operator for a tsunami source recovery, Siberian Electronic Mathematical Reports, vol. 11, pp. 532-547.

Voronin,V.V., Voronina,T.A., and Tcheverda,V.A.,(2015), Inversion method for initial tsunami waveform reconstruction, Nat. Hazards Earth Syst. Sci., vol. 15, pp. 1251-1263.

Voronina, T.A., Romanenko, A.A., (2016), The New Method of Tsunami Source Reconstruction With r-Solution Inversion Method. Pure and Applied Geophysics, 173(12), 4089 - 4099.

Voronina, T. A., Voronin, V. V. , Tcheverda, V.A., (2019) The 2015 Illapel Tsunami Source Recovery by Inversion of DART Tsunami Waveforms Using the R-Solution Method//Pure and Applied Geophysics, Springer Nature Switzerland AG, <https://doi.org/10.1007/s00024-019-02100-y>

Voronina T.A. and Voronin V.V., 2021 A Study of Implementation Features of the r-Solution Method for Tsunami Source Recovery in the Case of the Illapel Tsunami 2015, *Pure and Applied Geophysics*
<https://doi.org/10.1007/s00024-021-02843-7>

Mulia I E, Gusman A R & Satake K 2017 Optimal design for placements of tsunami observing systems to accurately characterize the inducing earthquake *Geophysical Research Letters* **44**
DOI: 10.1002/2017GL075791

The research proposed supported by the State Budget Program with ICMMG SB RAS
(0315-2021-0005)



Thank for your attention